

Performance-based methodology for assessing seismic vulnerability and capacity of buildings

Lin Shibin^{1†}, Xie Lili^{1,2‡}, Gong Maosheng^{1,2§} and Li Ming^{1,3†}

1. Institute of Engineering Mechanics, China Earthquake Administration, Harbin 150080, China

2. School of Civil Engineering, Harbin Institute of Technology, Harbin 150090, China

3. School of Civil Engineering, Shenyang Jianzhu University, Shenyang 11016, China

Abstract: This paper presents a performance-based methodology for the assessment of seismic vulnerability and capacity of buildings. The vulnerability assessment methodology is based on the HAZUS methodology and the improved capacity-demand-diagram method. The spectral displacement (S_d) of performance points on a capacity curve is used to estimate the damage level of a building. The relationship between S_d and peak ground acceleration (PGA) is established, and then a new vulnerability function is expressed in terms of PGA. Furthermore, the expected value of the seismic capacity index (SC_{ev}) is provided to estimate the seismic capacity of buildings based on the probability distribution of damage levels and the corresponding seismic capacity index. The results indicate that the proposed vulnerability methodology is able to assess seismic damage of a large number of building stock directly and quickly following an earthquake. The SC_{ev} provides an effective index to measure the seismic capacity of buildings and illustrate the relationship between the seismic capacity of buildings and seismic action. The estimated result is compared with damage surveys of the cities of Dujiangyan and Jiangyou in the M8.0 Wenchuan earthquake, revealing that the methodology is acceptable for seismic risk assessment and decision making. The primary reasons for discrepancies between the estimated results and the damage surveys are discussed.

Keywords: performance-based; vulnerability; building damage; seismic capacity; software HAZUS

1 Introduction

Seismic vulnerability assessment is vitally important for earthquake loss estimation and making seismic risk-management decisions. Several studies have proposed different vulnerability assessment methodologies using a variety of vulnerability parameters (Yin *et al.*, 1990; Singhal and Kiremidjian, 1996; Hwang *et al.*, 1997; Kircher *et al.*, 1997; Shinozuka *et al.* 2000; Porter *et al.*, 2001; Yakut *et al.*, 2006). Some representative methodologies are as follows. Yin *et al.* (1990) proposed a methodology that considers a shear strength for masonry buildings and an elongation ratio for RC frame buildings based on empirical data and theoretical analysis. Singhal and Kiremidjian (1996) used spectral acceleration to scale the vulnerability function based on nonlinear dynamic analysis. Shinozuka *et al.* (2000)

estimated the vulnerability parameters by the maximum likelihood method. Kircher *et al.* (1997) developed a building damage function in terms of spectral displacement by push-over analysis for the HAZUS project, named the HAZUS methodology in this paper. In some previous methodologies, the vulnerability analysis for building stock needs to be conducted individually for each building, which is hard and time-consuming to do for an entire city, while in the HAZUS methodology, all buildings in a city are represented by a limited number of model building types. The HAZUS vulnerability function uses a quantitative measurement of ground shaking instead of seismic intensity, and the methodology is based on push-over analysis rather than on empirical data, considering structural nonlinear performance by performance points as a single structure. Therefore, the HAZUS vulnerability assessment methodology is the most appropriate one to use for a performance-based vulnerability assessment of building stock.

The software HAZUS (Kircher *et al.*, 1997), developed by the National Institute of Building Sciences (NIBS) and the Federal Emergency Management Agency (FEMA), provides a powerful technique for earthquake loss estimation. However, it is so intimately connected to environments in the U.S. and seismic code that it is not easy to apply to other countries (Molina *et al.*, 2008). Moreover, the key to building damage estimation

Correspondence to: Lin Shibin, Institute of Engineering Mechanics, China Earthquake Administration, 29 Xuefu Road, Harbin 150080, China
Fax: +86-451-86664755
E-mail: shibinlin@gmail.com

[†]Graduate Student, [‡]Professor, [§]Associate Professor

Supported by: National Natural Science Foundation of China Under Grant No. 50908216; Postdoctoral Science Foundation of China Under Grant No. 20070420878

Received: June 25, 2009; **Accepted:** March 8, 2010

in HAZUS is the capacity-spectrum method (CSM), which is usually used for performance-based seismic analysis. The result of the assessment is presented in the form of S_d , so it has only an implicit physical meaning and cannot directly represent the seismic intensity directly. The iterative procedure is needed to determine a performance point, and does not always adequately converge. If the number of buildings is really large, this calculation is time-consuming. To solve these problems, this paper establishes a relationship between the S_d of the performance point and PGA of the corresponding response spectrum, then replaces S_d by PGA in the vulnerability function (Kircher *et al.*, 1997), and proposes a performance-based vulnerability assessment methodology, that can obtain the damage distribution quickly with high accuracy.

There is much research on estimating seismic damage (Yin *et al.*, 1990; Singhal and Kiremidjian, 1996; Hwang *et al.*, 1997; Tang and Chen, 2006; Wang and Xie, 2009), however, the meaning of the probability distribution of damage states and the difference between two different probability distributions has not been achieved. Furthermore, the relationship between seismic action and seismic capacity of the corresponding buildings is unknown. This paper presents SC_{ev} for assessing the seismic capacity of building stock. Some appropriate capacity curves and vulnerability parameters from *HAZUS-MH MR3 Technical Manual* are selected for estimation of building damage in China by comparing the seismic design spectrums of GBJ 11-89 and GB50011-2001 with UBC97. The seismic vulnerability and capacity of buildings in the cities of

Dujiangyan and Jiangyou in the 2008 M 8.0 Wenchuan earthquake are analyzed using performance-based assessment methodology, and the results are compared with seismic damage surveys (Zhang, 2008). Some remarkable conclusions are obtained.

2 Assessment of seismic vulnerability and capacity of buildings

2.1 HAZUS vulnerability assessment methodology

The model building types in HAZUS are classified based on the system presented in FEMA 178 (FEMA, 1992). Some building types are shown in Table 1. Each type represents a building stock with the same structure type and approximate height. Depending on the seismic design level and approximate age of construction, each type is divided into four seismic design levels: High-Code, Moderate-Code, Low-Code, and Pre-Code. Capacity curves and vulnerability parameters for each model type at one seismic design level are provided to estimate the seismic capacity of the building stock. Some typical vulnerability parameters and capacity curves are shown in Table 2 and Fig. 1, respectively.

The basis of the vulnerability assessment of HAZUS is CSM. The demand spectrum represents seismic action, which can be ascertained through the corresponding seismic design code. The initial demand spectrum is elastic, and the inelastic spectrum can be derived by introducing an effective damping and strength reduction factor. The capacity curve represents the

Table 1 Model building types (FEMA, 2003)

Building type label	Description	Height		
		Range		Typical Stories
		Name	Stories	
C3L	Concrete frame with unreinforced masonry infill walls	Low-rise	1–3	2
C3M		Mid-rise	4–7	5
C3H		High-rise	8+	12
URML	Unreinforced masonry bearing walls	Low-rise	1–2	1
URMM		Mid-rise	3+	3

Table 2 Vulnerability parameters of Low-Code (FEMA, 2003)

Parameter	Damage state	Building type				
		C3L	C3M	C3H	URML	URMM
Median: $S_{d,ds}$ (mm)	Slight	13.7	22.9	33	10.4	16
	Moderate	27.4	45.7	65.8	20.6	32
	Extensive	68.6	114.3	164.6	51.6	80
	Complete	160	266.7	384	120.1	186.7
Standard deviation, β_{ds}	Slight	1.09	0.85	0.71	0.99	0.91
	Moderate	1.07	0.83	0.74	1.05	0.92
	Extensive	1.08	0.79	0.9	1.1	0.87
	Complete	0.91	0.98	0.97	1.08	0.91

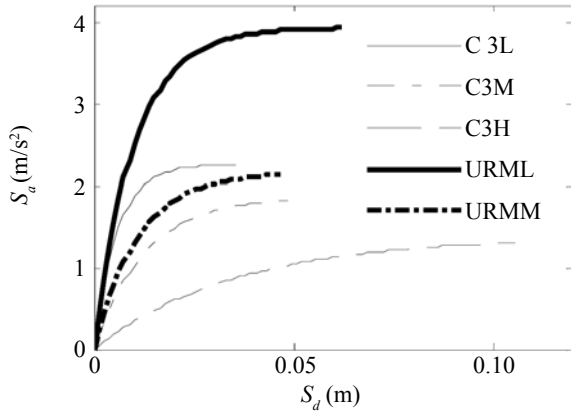


Fig. 1 Capacity curves of building model type of seismic design level, Low-Code (FEMA, 2003)

lateral resistance capacity of a building. By means of the iterative procedure, the intersection of the capacity curve and corresponding demand spectrum can be obtained, which is defined as a performance point. This point illustrates the seismic performance of the building under certain earthquake actions. The spectral displacement at the performance point is substituted into Eq. (1) to give the cumulative damage probabilities in different damage states. The vulnerability function has been developed by Kircher *et al.* (1997).

$$P[ds | S_d] = \phi\left[\frac{1}{\beta_{ds}} \ln\left(\frac{S_d}{S_{d,ds}}\right)\right] \quad (1)$$

where $S_{d,ds}$ is the median value of spectral displacement at which the building reaches the threshold of a damage state, ds ; β_{ds} is the standard deviation of the natural logarithm of spectral displacement for the damage state; and ϕ is the standard normal cumulative distribution function.

2.2 Improved vulnerability assessment methodology

The improved capacity-demand-diagram method is developed by Chopra and Goel (1999). This method uses a constant-ductility demand diagram for inelastic systems versus the elastic demand diagram in ATC-40 for equivalent linear systems. Combining the elastic demand spectrum with a $R_y-\mu-T_n$ relationship, the inelastic spectrum can be generated.

Zhuo and Fan (2001) developed the following $R_y-\mu-T_n$ expression based on a nonlinear time-history analysis program for inelastic single-degree-of-freedom (SDOF) systems:

$$R(T, \mu) = 1 + (\mu - 1) \times (1 - e^{-AT}) + \frac{\mu - 1}{f(\mu)} \times T \times e^{-BT} \quad (2)$$

where T and μ denote the natural period of the elastic SDOF system and ductility ratio, respectively. Function $f(\mu)$ and values of constants A and B that depend on the soil profile type are given in Table 3.

Table 3 Parameters of $R_y-\mu-T_n$ (Zhuo and Fan, 2001)

Soil Profile type	$f(\mu)$	A	B
I	$f(\mu)=0.80+0.90\mu$	4.84	0.40
II	$f(\mu)=0.76+0.09\mu-0.003\mu^2$	3.95	0.65
III	$f(\mu)=0.41+0.06\mu-0.003\mu^2$	1.38	0.87

In this study, the elastic design response spectrum in GB50011-2001 is used to determine the elastic demand spectrum, and then Eq. (2) is used to obtain the inelastic demand spectrum. The capacity curve, URML of Low-Code, is selected for the study of PGA and S_d . The procedure in the improved capacity-demand-diagram method is shown in Fig. 2.

Step1: Assume an initial PGA_0 and design response spectrum, Fig. 2 (a);

Step2: Convert the design response spectrum into elastic demand spectrum, and then into plastic demand spectrum, Fig. 2 (b);

Step3: Get a performance point via iterative procedure, Fig. 2 (c);

Step4: Plot PGA and the corresponding S_d at the performance point on a 2-D coordinate, Fig. 2 (d);

Repeat Steps 1 to 4 for an increased PGA to develop the required relationship between PGA and S_d .

The results in Fig. 2 (d) illustrate that the relationship between S_d of the performance point and PGA of the response spectrum is nearly linear, so it can be fitted by Eq. (3):

$$PGA = a \times S_d \quad (3)$$

where a is the slope of the fitted straight line, and S_d is the spectral displacement at the performance point. The validity and accuracy of Eq. (3) are examined in subsection 2.5. The linear relationship is fitted for the other four model buildings in Fig. 6, and the estimated results obtained by the two methodologies are presented in Fig. 7 to illustrate the feasibility of the proposed methodology.

Equation (3) can be used to transform Eq. (1) into Eq. (4), a function of PGA. Equations (1) and (4) show that β_{ds} is not influenced by the transformation. The cumulative damage probability can be obtained from Eq. (4) when the PGA is given, because the calculation for performance points is completed in advance and can be avoided from non-convergent phenomena. Moreover, the improved methodology is more efficient and straightforward in relating the seismic damage to seismic action.

The conditional probability of being in, or exceeding, a particular damage state, ds , given the peak ground acceleration, PGA, is defined by Eq. (4).

$$P[ds | PGA] = \phi\left[\frac{1}{\beta_{ds}} \ln\left(\frac{PGA}{PGA_{ds}}\right)\right] \quad (4)$$

where, PGA_{ds} is the median value of PGA at which the building reaches the threshold of a damage state, ds ; β_{ds}

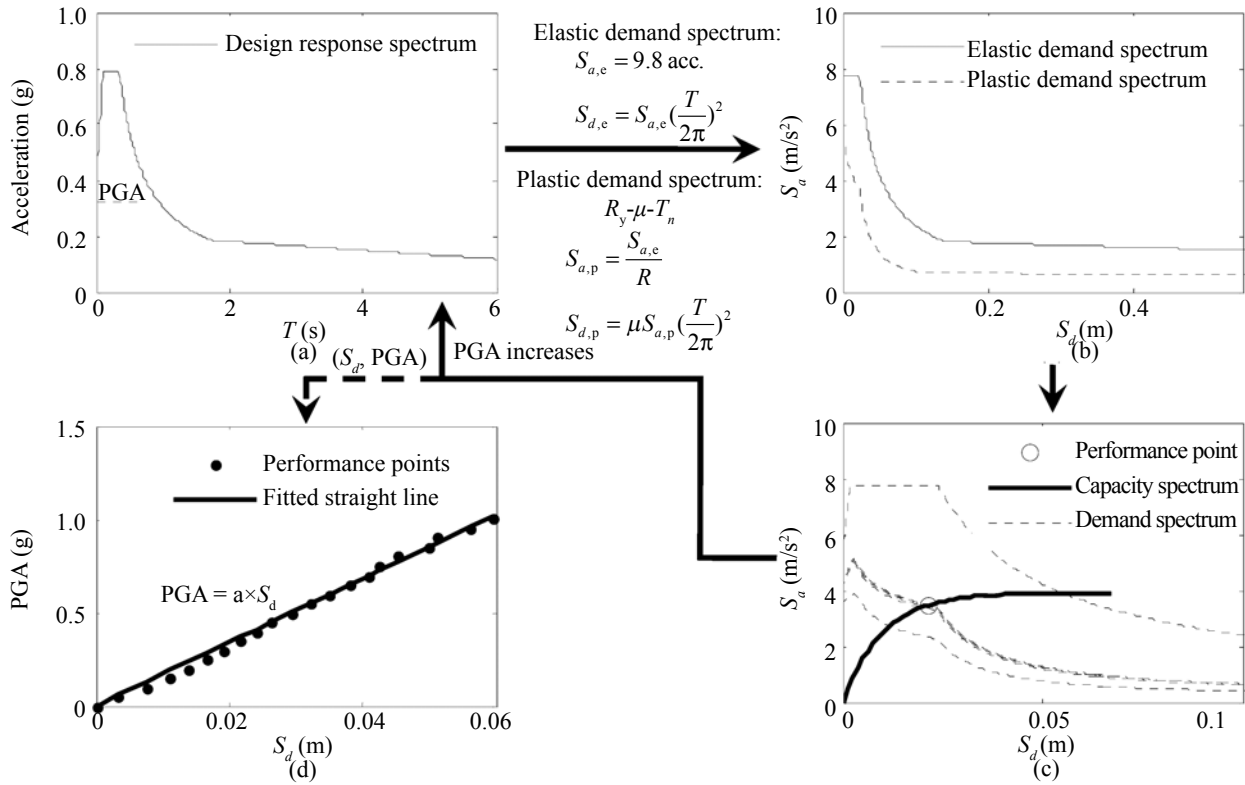


Fig. 2 Relationship between S_d of performance points and PGA of response spectra

and ϕ have the same definitions as in Eq. (1).

The probability of each structural damage state is given as a function of PGA:

$$\begin{aligned}
 P_{ds_i}(PGA) &= 1 - \phi\left[\frac{1}{\beta_{ds_i}} \ln\left(\frac{PGA}{PGA_{ds_i}}\right)\right] & i=1 \\
 &= \phi\left[\frac{1}{\beta_{ds_i}} \ln\left(\frac{PGA}{PGA_{ds_i}}\right)\right] - \phi\left[\frac{1}{\beta_{ds_{i-1}}} \ln\left(\frac{PGA}{PGA_{ds_{i-1}}}\right)\right] & 2 \leq i \leq 4 \\
 &= \phi\left[\frac{1}{\beta_{ds_i}} \ln\left(\frac{PGA}{PGA_{ds_i}}\right)\right] & i=5
 \end{aligned} \tag{5}$$

where i denotes a particular damage state for the building: None (1), Slight (2), Moderate (3), Extensive (4), Complete (5).

2.3 Seismic capacity assessment

The relationships between the damage index (DI) and seismic capacity index (SCI) of different damage states have been developed by Zhang *et al.* (2002):

The expected seismic capacity (SC_{ev}) is defined in terms of the probability distribution of damage states and the corresponding SCIs as:

$$SC_{ev} = \sum_{i=1}^5 SCI_{ds_i} \times P_{ds_i} \tag{6}$$

where, SCI_{ds_i} is the seismic capacity index and P_{ds_i} is the probability distribution of the i th damage states, ds_i .

Therefore, the expected SC_{ev} is used to characterize the seismic capacity of a building type with a given probability distribution of damage states. The flow chart of the seismic capacity assessment is shown in Fig. 3. The seismic capacity of the building type decreases as the seismic action intensity increases, as shown in Fig. 3 (d).

2.4 Comparing seismic design spectra of GBJ 11-89, GB50011-2001 with UBC97

In order to apply the HAZUS methodology to data obtained from China, the differences in structures

Table 4 Damage indexes and seismic capacity indexes for different damage states (Zhang, 2002)

Index	Damage state, ds_i				
	N(1)	S(2)	M(3)	E(4)	C(5)
DI	0	0.2	0.4	0.7	1
SCI	1	0.8	0.6	0.4	0.2

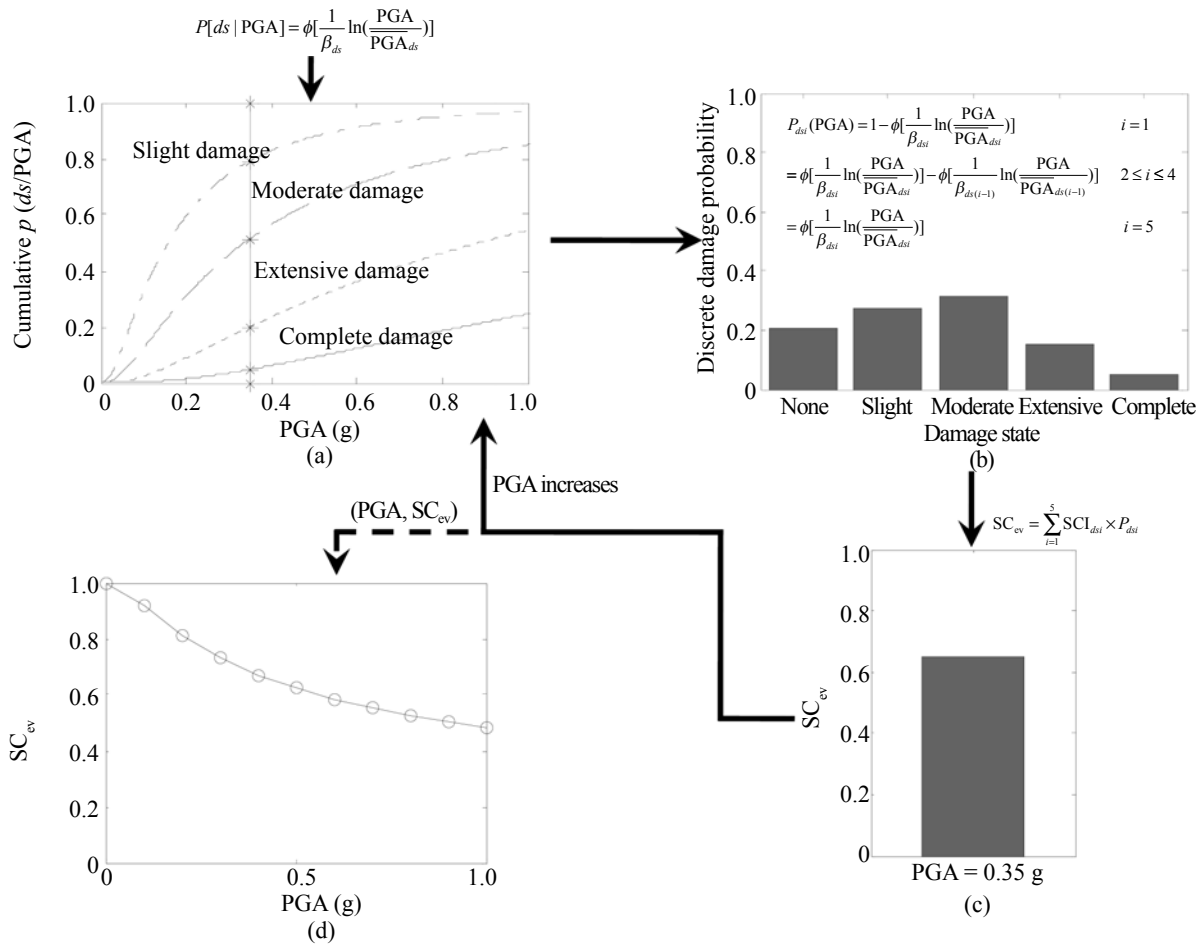


Fig. 3 Seismic capacity assessment flow chart

and seismic codes between the US and China have to be considered. This is a difficult task and somewhat imperfect. However, it provides a convenient and preliminary method to compare the seismic design spectra of the two countries.

In UBC 97, basic design ground motion has an exceedance probability of 10 % in 50 years. In order to satisfy the demand of ductile design, this code adopts R (numerical coefficient representative of the inherent overstrength and global ductility capacity of lateral force-resisting systems) to convert the original spectrum (10% in 50 years) to elastic design spectrum (63% in 50 years). Chinese seismic code adopts a three level seismic fortification criterion. At the first level (exceedance probability of 63% in 50 years) a strength check must be conducted for the structure of concern, then at the second level (10% in 50 years), seismic detailing should be incorporated into the design, and finally at the third level (2%–3% in 50 years), deformation requirements should be satisfied.

The seismic design load and standard load of UBC 97 have been compared by Sun and Wang (2007). To convert the design load to standard load, the factor of earthquake action, $F = 1.4$, is taken. The conversion of

the design response spectrum of UBC97 (design value) to the form of GB50011-2001 (standard value) is shown in Fig. 4.

The detailed procedure is as follows:

Step 1: Divide the original spectrum by R to get the design value of the elastic design spectrum;

Step 2: Divide the elastic design spectrum by F to obtain the standard value of the elastic design spectrum.

In UBC 97, for seismic zone 2A, assume a seismic

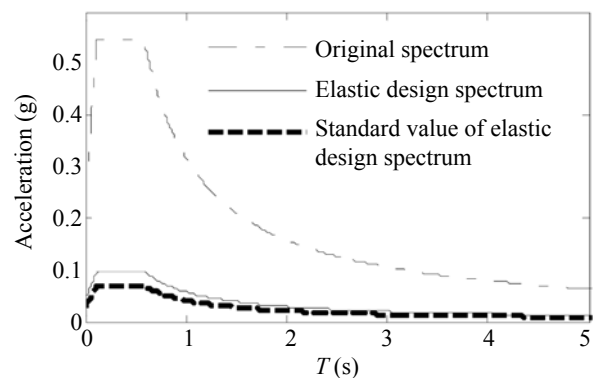


Fig. 4 Conversion of seismic design value to standard value

zone factor $Z = 0.15$, seismic coefficient: $C_a = 0.22$, $C_v = 0.32$; for seismic zone 1, assume: $Z = 0.075$, $C_a = 0.12$, $C_v = 0.18$, and soil profile types S_D (shear wave velocity 180–360 m/s), the response modification factor $R = 5.5$ for concrete intermediate moment-resisting frames and $R = 4.5$ for masonry bearing wall systems. Correspondingly, in GBJ 11-89 and GB50011-2001, assume a seismic fortification intensity VII, maximum influencing coefficient of horizontal seismic action is: 0.08 (63% in 50 years), soil profile types II (shear wave velocity 140–250 m/s), design characteristic period of ground motion $T_g = 0.35$ s in GB50011-2001 and $T_g = 0.3$ s in GBJ 11-89, and a damping ratio of 0.05. The design response spectra of UBC97 are converted and compared with the corresponding design spectra of GBJ 11-89 and GB50011-2001 as shown in Fig. 5.

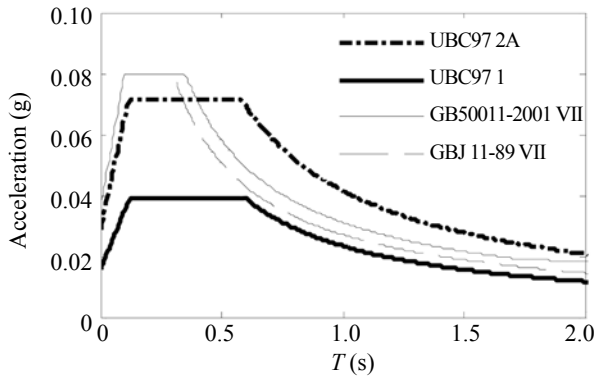
2.5 Selection and transformation vulnerability parameters

Seismic fortification intensity VII in GBJ 11-89 and GB50011-2001 is between UBC Seismic Zones 2A and 1, depending on the seismic design spectra to be compared. The classification of post-1975 buildings of HAZUS is Low-Code in UBC Seismic Zones 2A and 1. The capacity curves and vulnerability parameters of

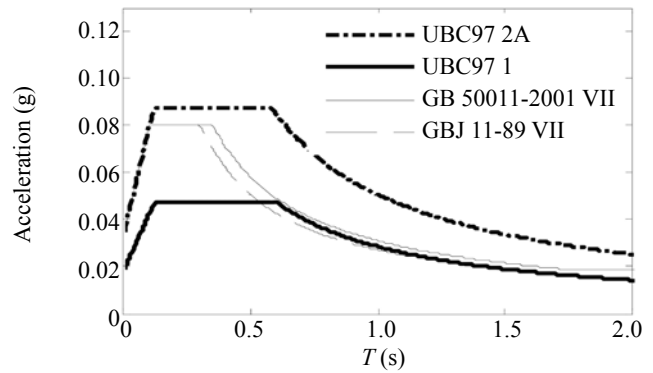
Low-Code in the *HAZUS-MH MR3 Technical Manual* are appropriate for the building damage estimation of building stock built after 1989 and in Chinese seismic fortification intensity VII zone. Depending on other comparisons of seismic design spectra and the seismic design level division of HAZUS, the division criterion of the seismic design level for Chinese buildings can be obtained to select capacity curves and vulnerability parameters by fortification intensity and building age. The divisions are listed in Table 5.

Five capacity curves for Low-Code shown in Fig. 1 are selected to establish the relationship between the PGA of the response spectrum and S_d for a performance point. The results are shown in Fig. 6. The slopes of fitted lines are listed in Table 6. The fitted slope of each model building type is substituted in Eq. (3) to transform the vulnerability parameters in Table 2 into the form of PGA. Table 7 lists the vulnerability parameters after transformation.

To verify the validity and accuracy of the improved vulnerability assessment methodology, the calculated damage probability distributions of five model building types with PGA of 350 Gal are calculated and compared with the original methodology as shown in Fig. 7. Note that the two show good agreement, indicating the feasibility of the transformation.



(a) Concrete intermediate moment-resisting frame system



(b) Masonry bearing wall system

Fig. 5 Comparison of design response spectrums in UBC97 and seismic fortification intensity VII in GBJ 11-89 and GB50011-2001

Table 5 Divisions of seismic design level for Chinese buildings

Fortification intensity	Built period		
	Pre-1978	1979–1989	Post-1989
IX (0.40g)	Pre-Code	Moderate-Code	High-Code
VIII (0.30g)	Pre-Code	Moderate-Code	Moderate-Code
VIII (0.20g)	Pre-Code	Low-Code	Moderate-Code
VII (0.15g)	Pre-Code	Low-Code	Low-Code
VII (0.10g)	Pre-Code	Pre-Code	Low-Code
VI (0.05g)	Pre-Code	Pre-Code	Pre-Code

Note: Figures in bracket denote the design basic PGAs.

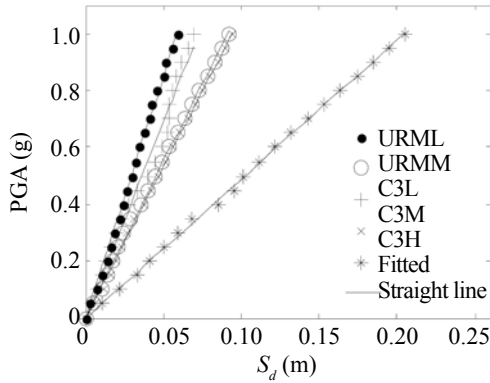


Fig. 6 Spectral displacement and PGA

3 Comparison of estimated and survey results for cities Dujiangyan and Jiangyou in M 8.0 great Wenchuan earthquake

Cities Dujiangyan and Jiangyou are located in Chinese seismic fortification intensity VII zone, the data and parameters of the Low-Code level are appropriate for their seismic damage estimation. Dujiangyan and Jiangyou are adjacent to the 350 Gal and 450 Gal contour line (Wang and Xie, 2009), respectively, and these two PGAs are used for seismic damage estimation in this paper.

Table 6 Slopes of fitted straight lines for different building types

Slope	Building type				
	C3L	C3M	C3H	URML	URMM
<i>a</i>	13.7941	10.6048	4.8851	17.0495	10.9666

Table 7 Vulnerability parameters for different building types of Low-Code level after transformation

Parameter	Damage state	Building type				
		C3L	C3M	C3H	URML	URMM
Median: PGA (g)	S	0.189	0.243	0.161	0.177	0.175
	M	0.378	0.485	0.321	0.351	0.351
	E	0.946	1.212	0.804	0.880	0.877
	C	2.207	2.828	1.876	2.048	2.047
Standard deviation, β_{ds}	S	1.09	0.85	0.71	0.99	0.91
	M	1.07	0.83	0.74	1.05	0.92
	E	1.08	0.79	0.9	1.1	0.87
	C	0.91	0.98	0.97	1.08	0.91

The damage state probabilities (P_{dsi}) in Dujiangyan and Jiangyou can be obtained using Eq. (5) with the given PGAs. The analytical results are listed in Table 8.

The numbers of different model building types (N_j) in Dujiangyan (Zhang, 2008) and Jiangyou are given in Table 9.

The N_j and $P_{dsi,j}$ are substituted in Eq. (7) to obtain the damage proportion for different building types, P_{dsi} , which is used to obtain the corresponding SC_{ex} values from Eq. (6).

$$P_{dsi} = \frac{\sum_{j=1}^n N_j \times P_{dsi,j}}{\sum_{j=1}^n N_j} \quad (7)$$

where, n represents the number of the model building types, in our case $n = 5$; and N_j is the number of the j th model building type. The estimated and surveyed results of damage proportion (P_{dsi}) and SC_{ev} are listed in Table 10.

The SC_{ev} provides an index to assess the seismic capacities of different building types and compares the different damage state probability distributions. Note that for RC frame buildings, the surveyed seismic capacity is higher than estimated, while for masonry bearing buildings the results show good agreement. In addition, the surveyed seismic capacity of RC frame buildings is much greater than for masonry bearing buildings, while the estimated RC frame buildings is only a little greater than for masonry bearing buildings.

There are many reasons for these differences

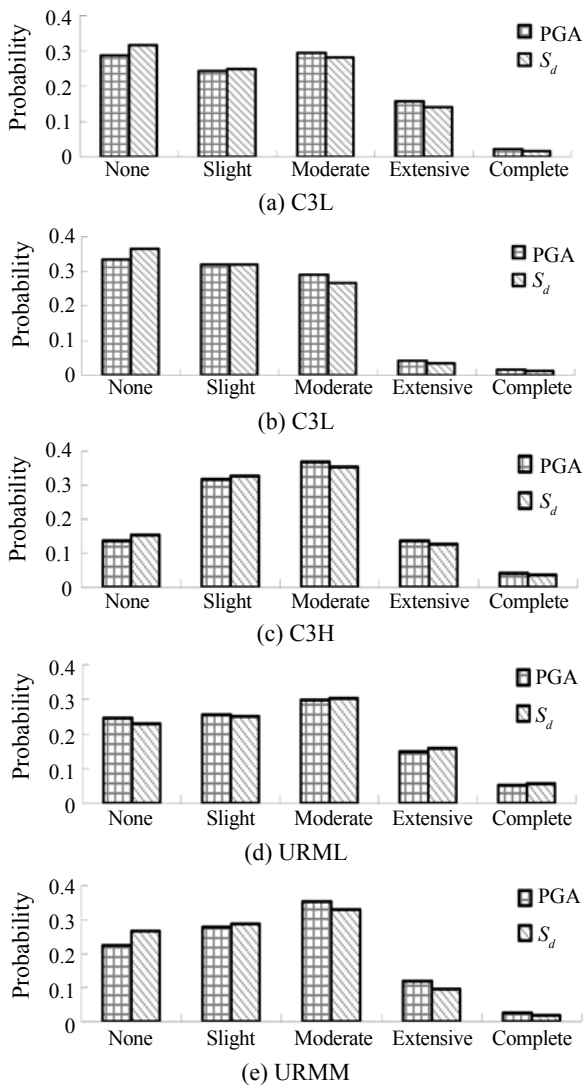


Fig. 7 Comparisons of damage probability distributions of the two methodologies

Table 8 Estimated damage state probabilities P_{dstj} of the two cities

Damage state	Building type				
	C3L	C3M	C3H	URML	URMM
N (1)	0.2859 <u>0.2130</u>	0.3336 <u>0.2340</u>	0.1374 <u>0.0741</u>	0.2461 <u>0.1734</u>	0.2240 <u>0.1503</u>
S (2)	0.2427 <u>0.2220</u>	0.3189 <u>0.3016</u>	0.3168 <u>0.2506</u>	0.2552 <u>0.2333</u>	0.2772 <u>0.2431</u>
M (3)	0.2928 <u>0.3191</u>	0.2896 <u>0.3595</u>	0.3681 <u>0.4158</u>	0.2976 <u>0.3222</u>	0.3534 <u>0.3851</u>
E (4)	0.1570 <u>0.2054</u>	0.0414 <u>0.0745</u>	0.1360 <u>0.1889</u>	0.1501 <u>0.1908</u>	0.1193 <u>0.1735</u>
C (5)	0.0215 <u>0.0403</u>	0.0165 <u>0.0303</u>	0.0417 <u>0.0705</u>	0.0510 <u>0.0803</u>	0.0261 <u>0.0480</u>

Note: For each damage state all upper figures are for Dujiangyan City, while all lowers with underlines for Jiangyou City.

Table 9 Numbers of different model building types (N_j)

City	Building type				
	C3L	C3M	C3H	URML	URMM
Dujiangyan	57	54	3	6	98
Jiangyou	62	57	10	783	1637

between the estimated and survey results. The analytical estimations do not include many in-situ conditions that may influence the analysis, such as infill walls, site and ground motion duration. Furthermore, practical damage surveys are mainly conducted by surveyors.

Table 10 Estimated and surveyed results of damage proportion (P_{dst}) and SC_{ev}

Structure type	Estimation						Survey					
	Damage state					SC_{ev}	Damage state					SC_{ev}
	N (1)	S (2)	M (3)	E (4)	C (5)		N (1)	S (2)	M (3)	E (4)	C (5)	
RC frame building	0.305	0.281	0.293	0.102	0.020	0.75	0.730	0.125	0.080	0.075	0.008	0.91
	<u>0.212</u>	<u>0.259</u>	<u>0.344</u>	<u>0.146</u>	<u>0.038</u>	<u>0.70</u>	<u>0.316</u>	<u>0.397</u>	<u>0.266</u>	<u>0.021</u>	<u>0.0</u>	<u>0.80</u>
Masonry bearing building	0.225	0.276	0.350	0.121	0.028	0.71	0.330	0.210	0.180	0.290	0.018	0.73
	<u>0.158</u>	<u>0.240</u>	<u>0.365</u>	<u>0.179</u>	<u>0.058</u>	<u>0.65</u>	<u>0.090</u>	<u>0.298</u>	<u>0.548</u>	<u>0.085</u>	<u>0.0</u>	<u>0.69</u>

Note: The top line presents the damage state for Dujiangyan (PGA=350 Gal), while the bottom line with underlines is for Jiangyou (PGA=450 Gal)

4 Conclusions

This paper uses the HAZUS methodology and the improved capacity-demand-diagram method to study the relationship between S_d and PGA, and then presents a performance-based vulnerability and capacity assessment methodology. Two cities that suffered severe damage in the 2008 Wenchuan earthquake, Dujiangyan

and Jiangyou, were used as examples. Seismic damage and capacity were estimated and compared with a corresponding survey of damage conducted after the earthquake. Some conclusions are summarized as below.

(1) The vulnerability assessment methodology is a quick and efficient way to assess the seismic damage of building stock based on seismic action (PGA) and model building types. The vulnerability function, in the

form of PGA, creates a significant relationship between building damage and ground motion characteristics. Furthermore, this function can consider the differences among buildings based on structure types, building heights, seismic design levels, and nonlinear responses.

(2) The seismic capacity SC_{ev} , an optimal estimation of seismic capacity and an effective index to measure the seismic capacity of a building type, shows the difference in probability distributions and can compare the seismic capacity of different building types. The relationship between the seismic capacity of buildings and seismic action is developed. Additionally, SC_{ev} provides a useful basis to assess the seismic capacity of an entire city.

Note that the vulnerability assessment methodology presented in this paper assumed that the model building types in HAZUS can represent the building stock, and then part(s) of them can be selected to estimate building damage and seismic capacity in China. The differences between US buildings and Chinese buildings were not substantially addressed in this paper.

Acknowledgement

Professors Zhang Minzheng and Sun Jingjiang at IEM, China Earthquake Administration, provided the seismic damage survey data. Dr. Sergio Molina at University of Alicante provided the capacity curves in HAZUS-MH. The author is grateful to all of them for their contributions to this study.

References

- Chinese Building Code (1989), *GBJ 11-89, Code for Seismic Design of Buildings (1989 Edition)*, Beijing: Chinese Building Industry Publisher. (in Chinese)
- Chinese Building Code (2001), *GB50011-2001, Code for Seismic Design of Buildings (2001 Edition)*, Beijing: Chinese Building Industry Publisher. (in Chinese)
- Chopra AK and Goel RK (1999), "Capacity-demand-diagram Methods Based on Inelastic Design Spectrum," *Journal of Earthquake Spectra*, **15**(4): 637–658.
- Federal Emergency Management Agency (FEMA), National Institute of Building Sciences (NIBS) *et al.* (2003), *HAZUS-MH MR3 Technical Manual*, Washington, D.C., www.fema.gov/hazus.
- Hwang HM, Lin H and Huo JR (1997), "Seismic Performance Evaluation of Fire Stations in Shelby County, Tennessee," *Journal of Earthquake Spectra*, **13**(4): 759–771.
- Kircher CA, Nassar AA, Kustu O and Holmes WT (1997), "Development of Building Damage Functions for Earthquake Loss Estimation," *Journal of Earthquake Spectra*, **13**(4): 663–681.
- Molina S, Lang DH and Lindholm CD (2008), *SELENA v3.5 User and Technical Manual*, NORSAR, www.norsar.no/pc-35-68-SELENA.aspx.
- Porter KA, Kiremidjian AS and LeCrué JS (2001), "Assembly-based Vulnerability of Buildings and Its Use in Performance Evaluation," *Journal of Earthquake Spectra*, **17**(2): 291–312.
- Shinozuka M, Feng MQ, Lee J and Naganuma T (2000), "Statistical Analysis of Fragility Curves," *Journal of Engineering Mechanics*, **126**(12): 1224–1231.
- Singhal A and Kiremidjian AS (1996), "Method for Probabilistic Evaluation of Seismic Structural Damage," *Journal of Structural Engineering*, **122**(12): 1459–1467.
- Sun X and Wang TH (2007), "Method for Conversion Seismic Load of UBC97 and GB50011-2001's," *Journal of Chemical Engineering Design*, **17**(4): 66–68. (in Chinese)
- Tang H and Chen GX (2006), "Building Seismic Damage Prediction Based on Coupling Model of GIS and BP ANN," *Journal of Xi'an University of Architecture & Technology (Natural Science Edition)*, **38**(4): 523–527. (in Chinese)
- Uniform Building Code (1997), *UBC 97, Code for Seismic Design of Buildings (1997 Edition)*, Structural Engineering Design Provisions, Vol.2.
- Wang W, Su JY, Ma DH, Han Y, Guo XD and Wang ZT (2008), "Approach to Earthquake Damage Prediction of Urban Buildings Based on Case Reasoning," *Journal of Xi'an University of Architecture & Technology (Natural Science Edition)*, **40**(2): 224–237. (in Chinese)
- Wang D and Xie LL (2009), "Attenuation of Peak Ground Accelerations from the Great Wenchuan Earthquake," *Earthquake Engineering and Engineering Vibration*, **8**(2): 179–188.
- Yakut A, Ozcebe G and Yucemen MS (2006), "Seismic Vulnerability Assessment Using Regional Empirical Data," *Earthquake Engineering and Structural Dynamics*, **35**(10): 1187–1202.
- Yin ZQ, Li SZ, Yan SW and ZZ (1990), "Estimating Method of Seismic Damage and Seismic Loss," *Journal of Earthquake Engineering and Engineering Vibration*, **10**(1): 99–108. (in Chinese)
- Zhang FH (2002), "The Study on Evaluation of Cities' Ability Reducing Earthquake Disaster," *Doctoral Dissertation*, Institute of Engineering Mechanics, China Earthquake Administration, Harbin, China. (in Chinese)
- Zhang MZ (2008), "Building Damage in Dujiangyan During Wenchuan Earthquake," *Earthquake Engineering and Engineering Vibration*, **7**(3): 263–269.
- Zhuo WD and Fan LC (2001), "On Strength Reduction Factors Used for Seismic Design of Structures," *Journal of Earthquake Engineering and Engineering Vibration*, **21**(1): 84–88. (in Chinese)